J Paleolimnol (2019) 62:373–388
https://doi.org/10.1007/s10933-019-00094-0

ORIGINAL PAPER

Water-level change recorded in Lake Pac Chen Quintana Roo, Mexico infers connection with the aquifer and response to Holocene sea-level rise and Classic Maya droughts

Anya Krywy-Janzen · Eduard Reinhardt · Chelsi McNeill-Jewer · Aaron Coutino · Brenda Waltham · Marek Stastna · Dominique Rissolo · Sam Meacham · Peter van Hengstum

Received: 24 October 2018 / Accepted: 3 September 2019 / Published online: 17 September 2019

Abstract Pac Chen Lake is located on the Yucatan Peninsula, Mexico and is ~ 42 km from the coast and ~ 22 km NE of Coba. It has an area of ~ 36,735 m^2 and maximum depth of 25 m. Four sediment cores along a depth transect provide a 4-ka record of the evolution of the eastern deep basin (core PC1 at 25 m depth) and the shallow margin (cores PC2–4 at 0.25–5 m depth). PC1 shows the effect of water-level rise and flooding of the shallow margin (2.8–1.8 ka) through a lithological (organic to carbonate) and geochemical (μXRF; decreased Ti, Fe, K and Ca) change along with a reduction in sediment accumulation (~ 0.2927 to 0.0343 cm $year^{-1}$). This change in sedimentation matches basal ages of PC2 and PC4 at 2.5 and 1.8 ka respectively, indicating water-level rise and flooding of the shallowly sloped margin which is within estimates of Holocene sea-level rise thus indicating connection with the aquifer. Corroborating evidence for connection with the aquifer comes from water-level monitoring (30 min intervals; 6 months December 12, 2018 to June 6, 2019) which shows a semi-diurnal tidal fluctuation (1–1.5 cm). Droughts have been thoroughly discussed as a proponent of the decline of the Classic Maya, with lakes being inferred to be isolated from the aquifer and experiencing water level drawdown. However, during the Classic Maya droughts lake drawdown in Pac Chen would be minimal, and there is no evidence of a water level drop in our lake margin stratigraphy (PC2–4). Water mass characteristics measured in March 2016 (temperature, conductivity) indicate some hydrological isolation from the aquifer. This isolation would have allowed for recording of environmental changes, but also likely changed through time as flooding of the

Electronic supplementary material The online version of this article (https://doi.org/10.1007/s10933-019-00094-0) contains supplementary material, which is available to authorized users.

A. Krywy-Janzen (✉) · E. Reinhardt · C. McNeill-Jewer
School of Geography and Earth Sciences, McMaster University, Hamilton, ON L8S 4K1, Canada
e-mail: krywyja@mcmaster.ca

A. Coutino · M. Stastna
Department of Applied Mathematics, University of Waterloo, Waterloo, ON N2L 3G1, Canada

B. Waltham
Department of Civil and Environmental Engineering, Carleton University, Ottawa, ON, Canada

D. Rissolo
Center of Interdisciplinary Science for Art - Architecture and Archeology, University of California-San Diego, San Diego, CA, USA

S. Meacham
CINDAQ - El Centro Investigador del Sistema Acuífero de Quintana Roo, A.C., Puerto Aventuras, Mexico

P. van Hengstum
Department of Oceanography, Texas A&M University, Galveston, TX 77553, USA

lake progressed. The shallow margin core PC4, however, recorded several rapid drops in K and Fe from ~ 1100 to 975, and 925–875 yr BP, which we interpret as periods of reduced inputs of terrigenous weathering during times of reduced rainfall and runoff. These periods are consistent with other regional paleoclimate records (lake and speleothem) of the Classic Maya droughts (1200–850 yr BP).

Keywords Yucatan · Lake level change · Hydrology · Aquifer · Sea level · Holocene · Classic Maya droughts

Introduction

The decline of the Classic Maya civilization is seen as a significant loss of human culture and history and a potential analogue to modern demographic collapses but involves a variety of complex human/environmental feedbacks (Brenner et al. 2001; Costanza et al. 2009). Droughts have been a prominent part of this discussion with a range of climate proxies being used from $\delta^{18}O$ records in speleothems and ostracods to sediment density (Hodell et al. 1995, 2005a, b; Curtis et al. 1996; Medina-Elizalde et al. 2010; Kennett et al. 2012; Douglas et al. 2016). Previous studies have inferred that northern lowland lakes are surficially closed, or effectively closed to the aquifer (leaky) through draping of sediment and thus are sensitive to changes in evaporation/precipitation (Curtis et al. 1996; Brenner et al. 2002; Hodell et al. 2005a, b). During periods of drought, lake-water level is thought to drawdown with evaporation and reduced rainfall, although the amount of drawdown or lake volume change has not been thoroughly quantified for northern lowland lakes (Brenner et al. 2002; Hodell et al. 2005a, b; Douglas et al. 2016). Recently Rosenmeier et al. (2016) modelled lake drawdown from $\delta^{18}O$ records from Lake Salpeten, Guatemala, but the lake is isolated, as it is at a higher elevation relative to groundwater. Pérez et al. (2010) used ostracods to identify Petén Itzá lake level fluctuations due to rainfall (< 500 yrs), but long-term lake level change has also been documented using seismic profiles and lithological changes (Hillesheim et al. 2005; Anselmetti et al. 2006). However, this hydrological isolation is not the necessarily the case for the northern lowland lakes of the peninsula where groundwater is closer to the surface (Brenner et al. 2002; Perry et al. 2003, 2009). Sea level is speculated to be a control on long-term lake-water level in the northern lowlands, but the relationship is undocumented even though it has been shown to be controlling groundwater elevation (Brenner et al. 2002; Collins et al. 2015).

Using data (testate amoebae; Ti, Fe, K) from radiocarbon dated sediment cores collected in the deep basin and shallow margin of Pac Chen along with recent water level monitoring, we investigate how long-term lake level is responding to Holocene sea-level rise and if Pac Chen is effectively closed from the aquifer, as lakes are previously been inferred to be, or if Pac Chen shows connection to the aquifer.

Yucatan climate and hydrology

The Yucatan Peninsula in Mexico is an expansive carbonate platform that separates the Gulf of Mexico and the Caribbean Sea. It is a tectonically stable, low-lying limestone/dolostone platform which has a Tertiary cover of highly porous and permeable rocks covering an area of approximately 165 000 km^2 (Ward et al. 1985). Mixing-zone hydrology, littoral processes and glacioeustacy have created a heavily karstified terrain with extensive cave systems, dissolution basins (aquadas) and sinkholes (cenotes; Beddows 2004; Smart et al. 2006). The Yucatan aquifer is temperature and density stratified like typical anchialine settings, with a meteoric water mass on top of a warmer marine water mass intruding from the coast (Beddows et al. 2007).

The climate of the Yucatan is similar to other Caribbean regions, with rainfall largely a result of the seasonal movement of the intertropical convergence zone (ITCZ). The ITCZ is the equatorial low-pressure belt that is comprised of the convergence of the Northern and Southern Hemisphere trade winds (Hastenrath and Polzin 2013). The north and southward movements of the ITCZ causes seasonal rainfall, with maximum levels occurring in early spring and late fall (Schneider et al. 2014). The dry season occurs December to April when the ITCZ is located farther south, which leads to a low seasonal rainfall of < 100 mm $month^{-1}$ on average (Negreros-Castillo et al. 2003). Conversely, the wet season occurs from May to November when the ITCZ has moved farther

north and causes increased rainfall of 1000–1500 mm month^{-1} (Metcalfe et al. 2015). This rainfall is in turn lost by evapotranspiration (85%) and infiltration to the aquifer through the porous karst which then flows towards the coast (Perry et al. 2003; Beddows 2004; Valle-Levinson et al. 2011; Null et al. 2014).

The hydraulic gradient of the aquifer is low due to the high karst porosity and predominance of large cave passages equating to a water table rise of 1–10 cm km^{-1} (Beddows 2004; Bauer-Gottwein et al. 2011). Water table elevations are relatively continuous following predicted trends inland except in the central hill district with its Cretaceous geology where there is likely a perched discontinuous aquifer. Variations in groundwater level and thus hydraulic gradient have been shown to vary with tidal (semi-diurnal) and seasonal (wet and dry) cycles as well as episodic large rainfall events (hurricanes, tropical storms). These water level changes vary in timing (days, weeks and months) and scale ($\sim$ <1 m), with short-term rainfall events causing the greatest change ($\sim$ 1 m) but only lasting for days to weeks due to the high hydraulic conductivity of Yucatan karst (10^4–10^5 m day^{-1}; Beddows 2004; Coutino et al. 2017; Kovacs et al. 2017b, 2018). Longer period seasonal changes are relatively small (< 0.5 m) but last for months during the wet and dry seasons, while over the long term, groundwater level has been shown to follow rising Holocene sea level (Collins et al. 2015; Smart et al. 2006).

Study site

Pac Chen is an enclosed freshwater lake consisting of three individual basins with an area of approximately 36,735 m^2, and is located in Quintana Roo, Mexico (Fig. 1). The basins likely originated as three collapsed caverns which have been subsequently infilled with sediment. It lies approximately 42 km from the coast and roughly 22 km NE of the archaeological site at Coba and approximately 6 km E from Punta Laguna. The shores are surrounded by wetlands and forest terrain with a village and an Alltournative Eco Tour Centre sit on the west side of the lake. The area surrounding the lake is relatively flat with a limestone topographic high ($\sim$ 10 m above lake level) at the SW corner of the lake where both the village of Pac Chen and the Alltournative facility are located. The bottom of Pac Chen has a continuous drape of sediment with no known cave passages connecting it to the aquifer. There are no significant archaeological sites surrounding Pac Chen but Coba is a large Late Classic period Maya city (1450–1150 yr BP) and Punta Laguna has a smaller Post-Classic site which is close by (Leyden et al. 1998).

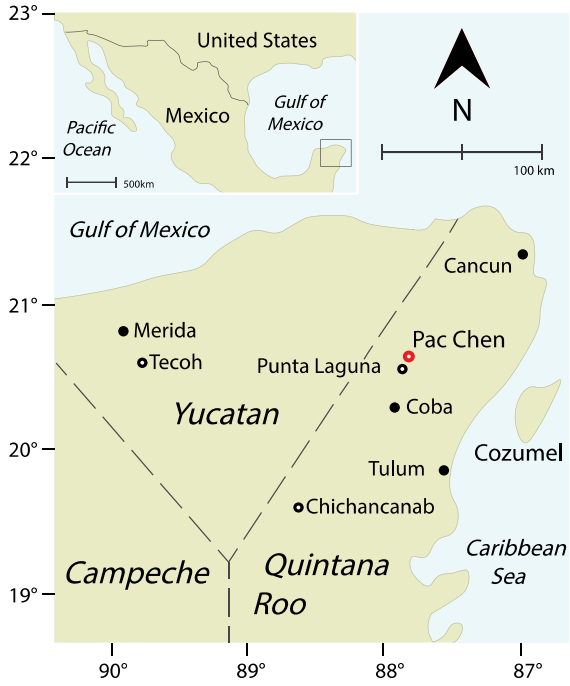

Fig. 1 Map showing the location of Pac Chen Lake (red circle) relative to cities (filled black circles) and sites with paleoclimate records (open black circles) referenced in the text. (Color figure online)

Materials and methods

Lake profile and depth measurements

A $\sim$ E–W depth profile was recorded using an Archer Field PC GPS receiver and a Vexilar LPS-1 Digital Handheld Depth Sounder which was calibrated with a weighted tape measure. A depth conductivity, temperature profile (0–15.5 m) was also measured at 1-m increments (March 2016) using a calibrated YSI Model 30 conductivity meter (1.0 µS cm^{-1} $\pm$ 0.5%; 0.1 °C$\pm$ 0.1 °C).

A HOBO® water-level sensor (U20L-04) was attached at $\sim$ 1.2 m water depth on a piling of the

dock located on the east side of the lake. Absolute atmospheric pressure was recorded with a HOBO® U20L-04 and corrected to water depth using the Barometric Compensation Assistant (± 0.5 cm; HOBOware PRO v3.7.8). Depth measurements were recorded every 30 min between December 12, 2018 and June 6, 2019.

Sediment core recovery

Four sediment cores were recovered in Pac Chen using Self-Contained Underwater Breathing Apparatus (SCUBA). PC1 was collected in the eastern basin at a depth of 25 m, and was 182 cm long. PC2, 3 and 4 were collected in a transect along the southwestern margin at depths of 5 m, 3 m and 0.5 m and are 66 cm, 86 cm and 98 cm long respectively (Fig. 2). Sediment compaction during coring was approximately 50% of the original penetration depth with PC2 and PC4 penetrating to refusal on underlying limestone. The surrounding topography was relatively flat around most of the lake basin, except on the SW corner where there is a topographic high (~ 10 m). PC2, 3 and 4 were collected here, as this location was deemed to be the most sensitive to recording terrigenous input from runoff versus the lower topographic areas surrounding the lake.

Core analytical methods

Element composition of the cores was analyzed using a Cox Analytical Systems Itrax µXRF core scanner at the McMaster Core Scanning Facility. Analysis used the Chromium heavy element (Cr-HE) X-ray source (30 kV, 10 mA, exp. time = 15 s, step-size = 500 µm). PC2, 3 and 4 were analyzed intact, while PC1 which was collected previously and sampled at 1-cm resolution was thus analyzed using the Sequential Sample Reservoir (SSR; Gregory et al. 2017b). Values were averaged over each analysis cell to produce a centimetre record of the core (Gregory et al. 2017b).

Microfossils (specifically, testate amoebae) were analyzed in PC1, 2 and 4 following the methods outlined in van Hengstum et al. (2008, 2010). Approximately 1.25 cm^3 samples were disaggregated and then wet sieved through a 45 µm screen to concentrate tests. Samples were subdivided into 8 aliquots using a wet splitter to achieve total specimen counts of ~ 100 where possible. Testate amoebae were identified using

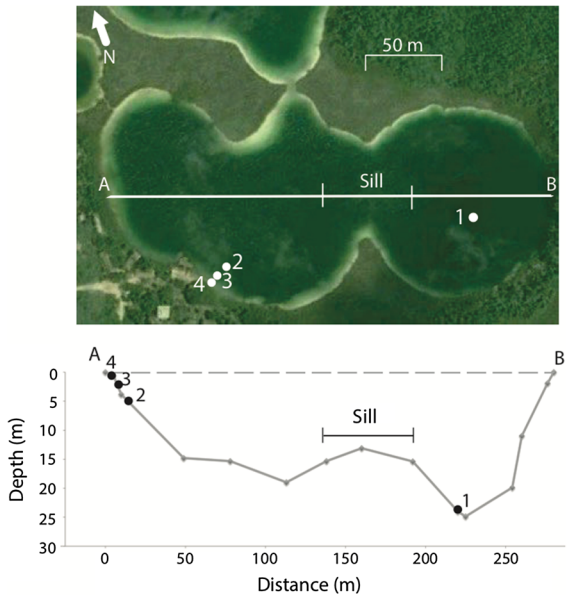

Fig. 2 Google Earth image of Pac Chen showing lake physiography with depth profile (m) and core locations. White line on Google Earth image denotes path of depth transect (cores were not taken along the transect but have been added to depth profile to show relative depths)

an Olympus SZX12 dissecting microscope (max. 135 X) and using taxonomy in van Hengstum et al. (2008). Data is represented as fractional abundances (%) of total counted specimens.

Twelve radiocarbon samples consisting of small twigs, charcoal or bulk organic matter (OM) were pretreated with acid/alkali/acid wash and analyzed by Direct AMS (Table 1). The R statistical software package Bacon 2.3 (Blaauw and Christen 2011) was used with the northern hemisphere calibration curve IntCal13 (Reimer et al. 2013) to calibrate raw radiocarbon ages as ranges in calibrated years before present (cal yrs BP) with a 95% confidence interval. An age model was fit to the data and interpolated ages were calculated at 1-cm (PC1) and 500-µm (PC2–4) intervals. Calibrated yr BP are used unless otherwise noted.

Results

Water body characteristics

Surface water in Pac Chen has a measured salinity of 0.5 ppt with a thermocline at ~ 5 m where there is a

Table 1 Radiocarbon results from PC1–4

Core no.	Lab ID D-AMS	cm	Material	$\delta(^{13}C)$ (per mil)	^{14}C age ($\pm$ 1σ yr BP)	Cal yr BP (2σ)
1	8976	18.5	OM	− 34.6	1273 ± 24	1275–1179
	8977	36.5	OM	− 37.6	1788 ± 27	1814–1689
	8362	60.5	OM	− 31.6	1891 ± 23	1890–1777
	8363	120.5	OM	− 32.4	2403 ± 27	2491–2351
	8365	180.5	OM	− 28.9	3717 ± 27	4104–3982
2	13,073	3.5	OM	− 27.8	1970 ± 30	1992–1868
	13,074	51.5	Twig	− 24.9	2535 ± 29	2596–2496
3	13,078	54.5	Twig	− 25.9	857 ± 23	796–701
4	13,071	19	Twig	− 23.3	367 ± 24	498–426
	13,072	50.5	Twig	− 27.6	1153 ± 24	1150–1044
	13,077	76.5	Charcoal	− 16.9	1825 ± 24	1823–1706
	13,070	94	Twig	− 23.3	1876 ± 26	1877–1734

Dates were calibrated using northern hemisphere calibration curve IntCal13 (Reimer et al. 2013)

$\sim$ 3 °C drop in temperature and specific conductivity (SEC $\sim$ 40 µS cm^{-1}; Fig. 3).

The water depth measured from December 2018 to June 2019 shows tidal water-level changes in Pac Chen (Fig. 4). A semi-diurnal tidal variation is evident with regular periodicity, showing an $\sim$ 1 to 1.5 cm change in water depth with amplitudes of $\sim$ 12 to 13 h which matches the M_2 tidal constituent of 12.42 h (Fig. 4; Talley et al. 2011). Tidal measurements at Puerto Morelos show a similar semi-diurnal tidal periodicity with an $\sim$ 10 to 20 cm range which is also observed in groundwater level ($\sim$ 10 to 12 cm; Parra et al. 2015; Kovacs et al. 2017b). There are periods where the water depth departs from this semi-diurnal periodicity, which may be from wave action, but also rainfall events which is evident from Feb $\sim$ 12 to 15, 2019 when water level rose by 5 cm and then gradually fell over three days. The Pac Chen record also shows an overall drop in water level ($\sim$ 50 cm) as the dry season progresses which is a similar pattern and magnitude recoded in groundwater levels (Kovacs et al. 2017b, 2018). Longer term monitoring of water level in Pac Chen will further document seasonal relationships.

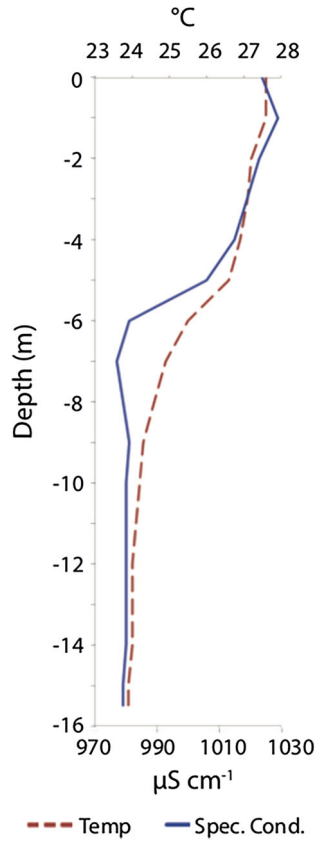

Fig. 3 Temperature (°C) and specific conductivity (µS/cm) profile showing upper thermocline in the lake which was measured at the PC1 location (Fig. 2)

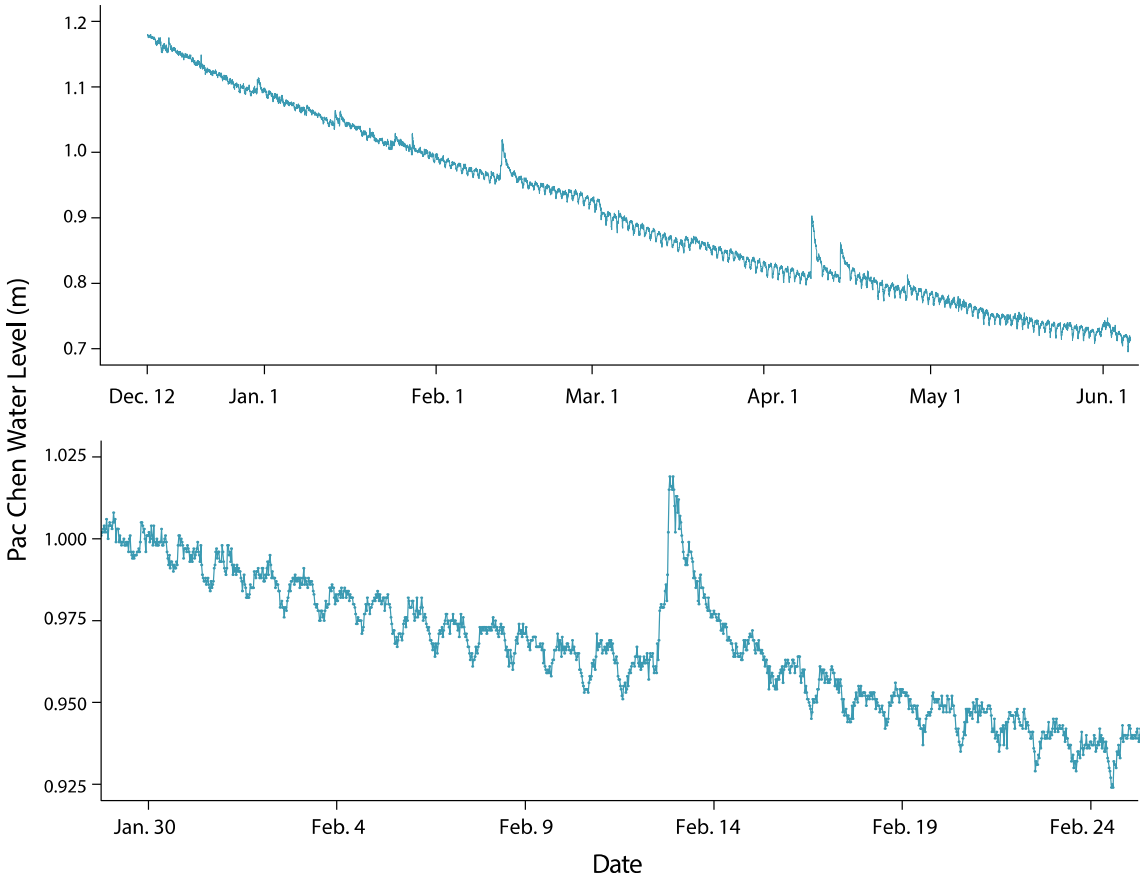

Fig. 4 Water-level data from Pac Chen Lake. Data covers December 12/18 to June 6/19 (top profile) and bottom profile shows January 30 to February 24

Sediment cores

Core lithology

PC1 was from the deep basin (− 25 m) and contains dark, fine-grained OM (organic matter; 185–120 cm) with increased carbonate content (marl and shells) towards the top of the core (120–0 cm). Intact and fragmented gastropods are found throughout the core as well as wood and leaf fragments (ESM1). PC2 which was collected at − 5 m depth and is composed of marl and fine OM with distinct beds of higher or lower OM content (e.g. 50 and 29 cm; Fig. 5). Intact and fragmented gastropods are also present, but to a lesser extent than the other cores. PC3 and PC4 which were collected at − 3 and − 0.5 m water depth, also contain marl and fine OM, but also have a bed of coarser OM and gastropod shells from ∼ 63 to 52 cm in PC 3 and ∼ 50 to 40 cm in PC4 (ESM3, 4). PC4 also has OM rich units at ∼ 12–9, 22–16 and 95–91 cm.

Age models

Radiocarbon ages show no reversals with a basal age of 4104–3982 yr BP in PC1 and 1877–1434 yr BP in PC4 (ESM6; Table 1). The age models for PC1 to 4 are generally linear with some changes in accumulation rates. PC 1 has relatively high accumulation rates between ∼ 181 and 37 cm (0.0370–0.2927 cm year^{-1}) with lower accumulation rates from ∼ 37 to 0 cm (0.0144–0.0343 cm year^{-1}). The average rate over the entire length of the core (181 cm) is 0.097 cm year^{-1}. In PC 4, the accumulation rate from 77 to 0 cm was ∼ 0.04 cm year^{-1} and higher from 94 to 77 cm (0.40 cm year^{-1}). The average accumulation rate in PC4 (0.14 cm year^{-1}) was ∼ 1.5 X higher than PC1.

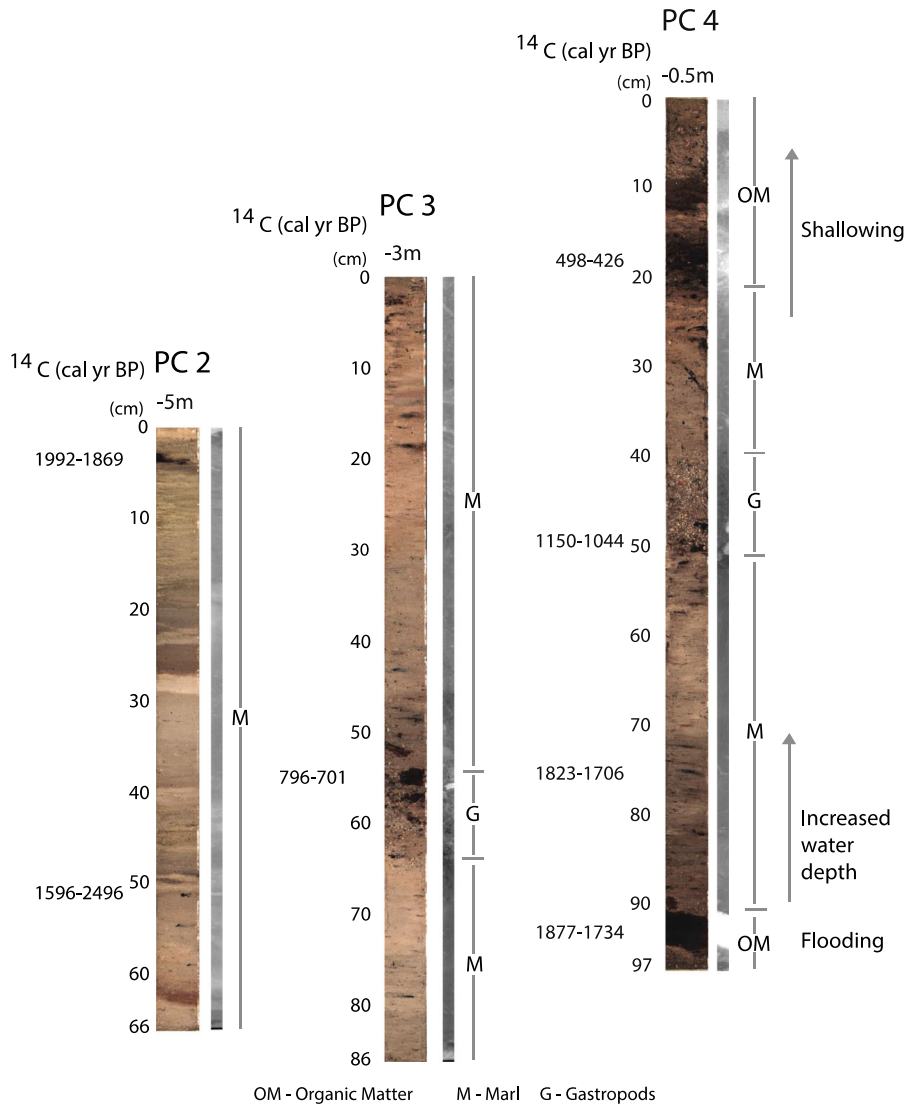

Fig. 5 Details of PC2, 3 and 4 core stratigraphy (RBG and radiographic images) with calibrated radiocarbon ages (cal yr BP), water depths (m) and lithological composition. (Color figure onlline)

µXRF records

The PC1 records for Ti, Fe, K show similar trends spanning the last ∼ 4 ka. Values are relatively high from ∼ 4 to 2.5 ka and then decline until ∼ 1.8 ka after which they remain relatively constant albeit with a slight reduction until present. Calcium shows the opposite trend increasing over the past ∼ 4 ka but with similar inflection points as Ti, Fe and K. The increase in Ca at ∼ 2.5 ka matches changes in sediment color, with lighter colours representing higher carbonate (shells and marl) versus OM content. The Inc/Coh values which can be a measure of OM content and porosity of the sediment are inversely correlated with Ca but show only minor trends with Fe, Ti and K (Fig. 6, ESM5; Jouve et al. 2013).

Cores from the shallow margin of Pac Chen (PC2, 3, 4) share similar results in their Ti, Fe, K records, but they are lower in magnitude relative to PC1 and the overall variation in values is not as great (ESM2, 3, 4). Ti, Fe and K all co-vary in the cores, except K in PC3, which does differ slightly in occurrence of inflection points and peaks in the record compared to Ti and Fe. PC3 and 4 have overall decreasing trends in Ti, Fe, K. Ca and Inc/Coh also show similar relationships as described for PC1, but do not vary to the same extent, since the sediment is more homogeneous being composed of a gradation of marls and OM compared

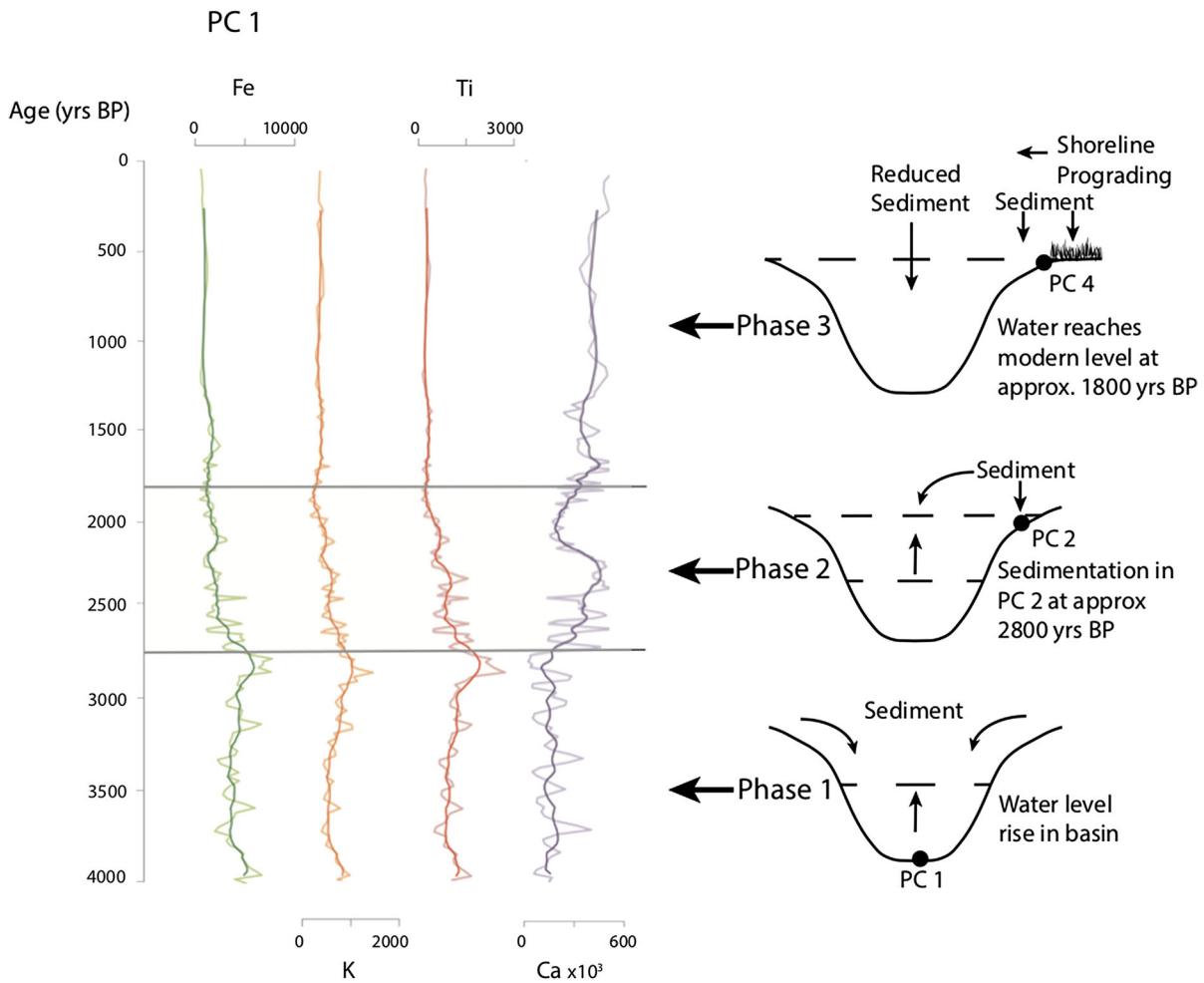

Fig. 6 Lithological transitions (Fe, K, Ti, Ca) in PC1 plotted relative to calibrated yr BP. Flooding evolution based on these transitions are also shown, including the basal ages (cal yr BP) of PC2 and PC4

to PC1, which has intervals with higher OM/carbonate content. There are two gastropod concentrations in PC3 (63–56 cm) and PC4 (50–40 cm), but otherwise are largely undifferentiated marls and OM. PC4 has an OM unit at the base and has higher OM contents at the top of the core relative to PC3, but otherwise all the shallow margin cores share similar lithologies.

Microfaunal assemblages

In PC 1, *Centropyxis aculeata, Centropyxis constricta* were the dominant taxa with *Difflugia oblonga* present only in minor abundance ($\lesssim$ 5%) along with two additional undifferentiated taxa which were also minor (ESM1). In PC2 and 4, the dominant taxa was *C. aculeata* with minor abundance of *C. constricta* and there was no clear trend in the cores (ESM2, 4). Overall, the testate amoebae data is unchanging in the cores with only a minor change in PC1 from 40 to 0 cm. The low-diversity assemblage is indicative of a low-salinity stressed environment (van Hengstum et al. 2008; Regalado et al. 2018).

Discussion

Long-term lake-level and sea-level rise

Based on the evidence in the sediment cores, there is a progression of flooding that appears to match Holocene sea-level rise and thus has important implications for connectivity of the lake to the aquifer.

Evidence for this flooding sequence is from the change in sediment rate and composition found in the deep basin core PC1 and the basal age of the shallow margin core PC4 (Fig. 6).

If the lake is connected to the aquifer as we surmise, and the aquifer is in turn responding to sea-level rise as has been demonstrated in previous studies, the bottom of the lake would have been flooded by at least ~ 11 to 10 ka. Our basal age for PC1 is ~ 4 ka, so water level was already at ~ − 2 to − 3 m below present at this stage, but may have been closer to − 5 m. The near basal age of PC2 which was collected at ~ − 5 m is ~ 2.5 ka indicating that the water level was at this point in time, but perhaps earlier, because there is no age for the bottom of the core, and this elevation may have been flooded but not accreting sediment prior to this date. This lack of sediment accumulation with water-level rise has been noted in previous studies which examined groundwater elevation and Holocene sea-level rise in cave sediments (Collins et al. 2015). The sill separating the two deep basins was connected by ~ 2.5 ka but the areal extent of the lake was slightly smaller than present. Holocene sea level had already begun its deceleration at ~ 7 to 6 ka, but the slowed water-level rise after 2.5 ka allowed wetlands to develop (ESM7; Khan et al. 2017). These fringing wetlands began baffling and accreting sediments on the shallowly sloped margin reducing sediment input to the deep basin. This change in the loci of sedimentation is evidenced by the higher amount of terrigenous elements (Ti, Fe and K) in the basal portion of PC1 relative to the top, and the decrease in sediment accumulation at ~ 1.8 ka (PC4).

This timing for the change in sedimentation in PC1 corresponds to the age for the flooding and accretion of sediments on the shallow lake margin (PC4), which occurred at ~ 1.8 ka which is consistent with the rate and magnitude of Holocene sea-level rise. However, the change in sediment composition (Ti, Fe and K) in PC1 also coincides with increased carbonate content of the sediment (Ca) and decreased Inc/Coh values, so the decrease in Ti, Fe and K is also a matrix effect with μXRF analysis. However, the increased carbonate content in PC1 likely originates from this newly created biogenic production in the shallow wetland with the rising water-level after 2.5 ka and thus records changing sediment sources with water-level rise. The testate amoebae assemblage in PC 1 also changes during this interval (40–0 cm) with increased amounts of *D. oblonga* which may be due to reduced OM content and oxygenation of the sediment/water interface, or more likely *D. oblonga* is being transported downslope from the shallow margin which forms with rising water level. *D. oblonga* is not found in our shallow cores (PC2–4) but they may exist on the margins of the eastern basin. A similar trend was found in Little Spring in Florida, where flooding of the shallow sloped margin caused wetland development and increased OM deposition in the deep basin (Gregory et al. 2017a). Sediment accumulation in PC2, which is at − 5 m depth, stops at ~ 1.9 ka which is close to the timing for the onset of sedimentation in PC4 at ~ 1.8 ka. This also indicates preferential trapping of sediment in the lake margin wetlands.

Open, leaky or closed?

The progression of flooding and its effect on sedimentation over the past ~ 4 ka in Pac Chen suggests that the lake is connected to the aquifer and is responding to sea-level rise. Presently, the water level in Pac Chen shows a semi-diurnal tidal pattern with a 1–1.5 cm amplitude, and a similar tidal pattern has been found in long-term monitoring of groundwater level in nearby cave systems, but the amplitude in Pac Chen at 43 km inland seems high (Coutino et al. 2017; Kovacs et al. 2017b). Tidal amplitude in unconfined-porous medium aquifers like that of the Yucatan, theoretically decreases exponentially moving inland (Fetter 1988). Beddows (2004) measured tidal amplitude attenuation in several cenotes at Nohoch Nah Chich noting that values deviated significantly from theoretical values. At ~ 10 km inland, ocean tide amplitude should be reduced to 8.6% but actual measurements from Nohoch were higher at 16%. This departure from theoretical values is likely due to the connection between the aquifer and ocean via large cave conduits (passages; Beddows 2004). So although the tidal amplitude in Pac Chen is high versus theoretical values (1–1.5 cm; < 1 cm) it is not unexpected, and will require further research to explain, but the semi-diurnal periodicity as well as rapid draining after large rainfall events does indicate connection with the aquifer.

Despite this connection with the aquifer, it also appears that the lake is hydrologically isolated in terms

of interchange between the two water bodies (Curtis et al. 1996; Hodell et al. 2005a). It is unclear how much interchange occurs, but there seems to be a significant residence time of water in the lake since there is a distinct thermocline at − 6 m and the bottom water temperature is ∼ 24 °C while groundwater temperatures are ∼ 25 °C (Kovacs et al. 2018; Coutino et al. 2017; Beddows 2004). These groundwater temperatures in the meteoric water mass have been recorded closer to the coast, but the 1 °C cooler temperature suggests that there is only limited interchange between lake and groundwater. Rainwater is generally cooler, which has been observed to reduce aquifer temperatures after large events, so it is likely the lake water is largely derived from rainfall (Kovacs et al. 2018). The presence of a thermocline and increased conductivity of surface water due to evaporation also indicates limited interchange, although thermoclines are also found in cenote water bodies as well (Beddows 2004). Collectively, present water conditions in Pac Chen indicate that water level is responding to tidal fluctuations but is a separate water body (hydrologically isolated or leaky) and thus affected by seasonal changes in evaporation and rainfall.

However, over the long term, sea level appears to be controlling lake-water level and the degree of interchange with the aquifer as surrounding karst is flooded is unknown. This is especially true before sediment begins to blanket the basin margins occluding the highly porous limestone. Therefore, caution should be used when interpreting long term paleoclimatic records in the northern lowland lakes, as the lakes may vary between open, leaky and closed with Holocene sea-level rise (Perry et al. 2009).

Lake water drawdown during Classic Maya droughts

Previous lake studies examining paleoclimatic records of the Classic Maya droughts in the northern lowlands have referred to lake level drawdown during this period. This is predicated on the lakes being closed or leaky basins (Curtis et al. 1996; Brenner et al. 2002; Hodell et al. 2005b). However, there have been no studies examining lake margin stratigraphic records testing this hypothesis. Based on our previous discussion regarding lake connectivity to the aquifer with sea-level rise, there would be no significant water-level drop during droughts. Groundwater level, and thus Pac Chen lake level, will be largely controlled by sea level because of the anchialine hydrology and the high hydraulic conductivity of Yucatan karst (Fig. 7; Collins et al. 2015). During extended dry periods, groundwater level would be lower as observed in groundwater monitoring studies showing seasonal changes corresponding to a thinner meteoric water mass (< 0.5 m; Kovacs et al. 2017b, 2018). However, during extended dry periods (years) it would be expected that seawater would intrude from the coast replacing the missing freshwater. The hydraulic gradient would be affected by the thinner meteoric water mass, but it would be minor, resulting in little net change of water level (Kovacs et al. 2017b). Therefore, if Pac Chen is connected to the aquifer, lake level during the Classic Maya droughts would only experience a minor drawdown.

This lack of drawdown during the Maya droughts is reinforced by our lake margin stratigraphy (PC2–4; Fig. 5). PC4 which is the shallowest core (− 0.25 m) shows OM at the base, which likely represents a shallow wetland as the karst is initially flooded, followed by an interval of carbonate mud indicative of deeper water and then an increase in OM towards the top of the core as sedimentation infills the reducing accommodation space causing shallowing. The only notable interval within this sequence of sediments is the gastropod shell layer (∼ 50 to 40 cm) which dates (∼ 1150 to 1050 yr BP) to the Maya droughts (1200–850 yr BP), but doesn't appear to be related to water depth (Hodell et al. 2005a). Gastropods don't dominate the upper portion of PC4 which is at − 0.5 m and observations of the modern surface found no existing concentrations. PC3 is more carbonate mud rich, suggestive of deeper conditions as the core was collected at − 3 m and further away from the fringing wetland vegetation. Again, the only notable feature is another gastropod layer (∼ 63 to 56 cm) with slightly higher OM contents, which has a younger age to that in PC4 (∼ 800 to 700 yr BP), but does not date to the period of droughts (1200–850 yr BP). The gastropod layer in PC4 could be interpreted as a slight decrease in water depth during the time of the droughts (< 0.5 m), which may be the case, but there is no evidence of subaerial exposure. No depositional hiatuses or roots, indicating a water level drop are observed. Nor are there indurated or cemented layers which can occur with subaerial exposure in carbonate mud rich sediments. While it

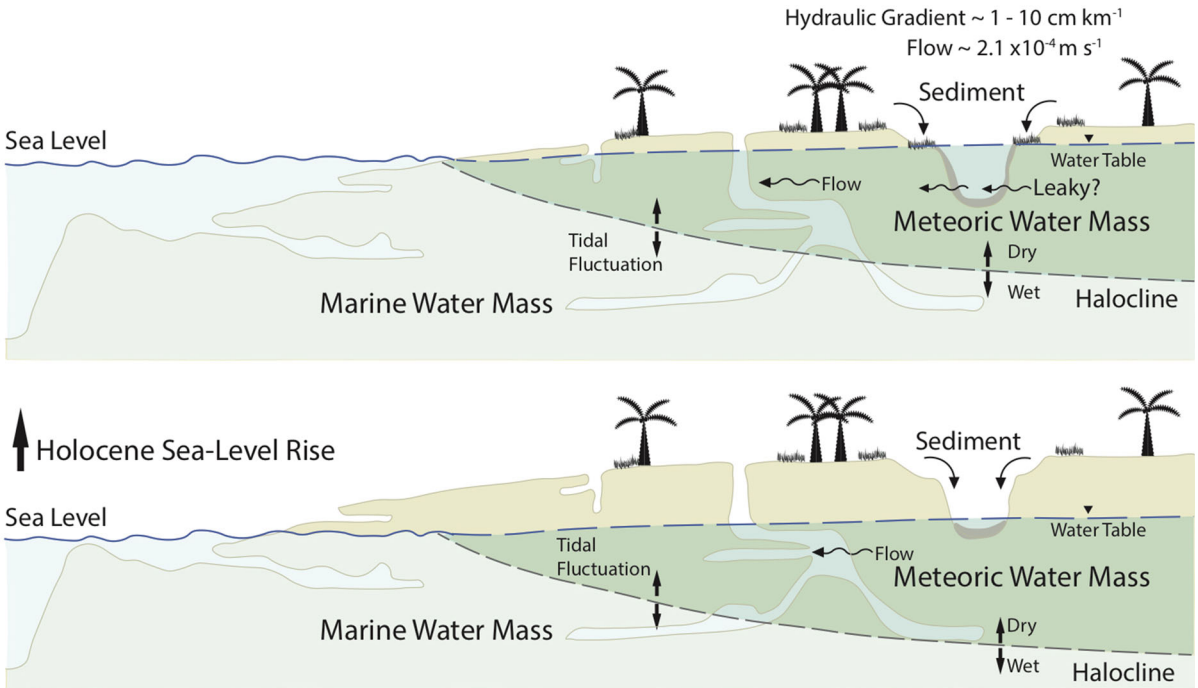

Fig. 7 Diagrammatic evolution of Yucatan aquifer with Holocene sea-level rise. Marine and meteoric water masses are depicted and movement of the halocline with tidal fluctuations and relative wet versus dry climates

is true that the concentration of gastropods may relate to changing salinity or other ecological effects of the droughts, the gastropod layers don't appear to be reliable indicator of changing water depth. There is also no change in the testate amoebae over this time interval, in terms of water depth or salinity change, although the stressed *Centropyxis* spp. dominated assemblage is likely not sensitive enough to record these changes (Regalado et al. 2018; van Hengstum et al. 2018). Based on this evidence, at least in Pac Chen, the water level during the droughts doesn't seem to have been significantly lower, and the lake would have largely remained at its current size in terms of areal extent.

Potassium record of the Classic Maya droughts

PC2–4 have relatively consistent lithologies, with higher sediment accumulation rates and PC4's location closest to the source of karst weathering input from the topographic high makes it the best to record climatic effects.

Fe, Ti and K show direct interrelationships in PC4, but the Ti record in PC4 is not as useful as Fe and K, because its concentration is not high enough in portions of the core. Fe and K however, are within the detection limits of the μXRF and co-vary with only minor differences. There is an indirect relationship between K and Inc/Coh in PC2–4, but also a large spread in values, and Fe shows little relationship with Inc/Coh. However, Fe and K both still share a similar trend in the cores. Potassium is likely more affected by changes in OM content in the sediment because of the secondary plant source, while Fe will be less so, because the source of the latter is largely from lithogenic weathering of limestone and aeolian dust. So, there is an overall minor matrix effect with K which is in part OM dependent. Nevertheless, the K trend towards lower values towards the top of PC4 seems to be a primary environmental signal as it is replicated in the Fe record. Fe may be affected by redox diagenesis, while Ti and K will be unaffected by post depositional migration within the sediment, although this doesn't appear to be significant as Fe covaries similarly with K and Ti (McNeill-Jewer et al. 2019).

Because the Yucatan peninsula is composed of limestone, there is little siliciclastic sediment as an Fe

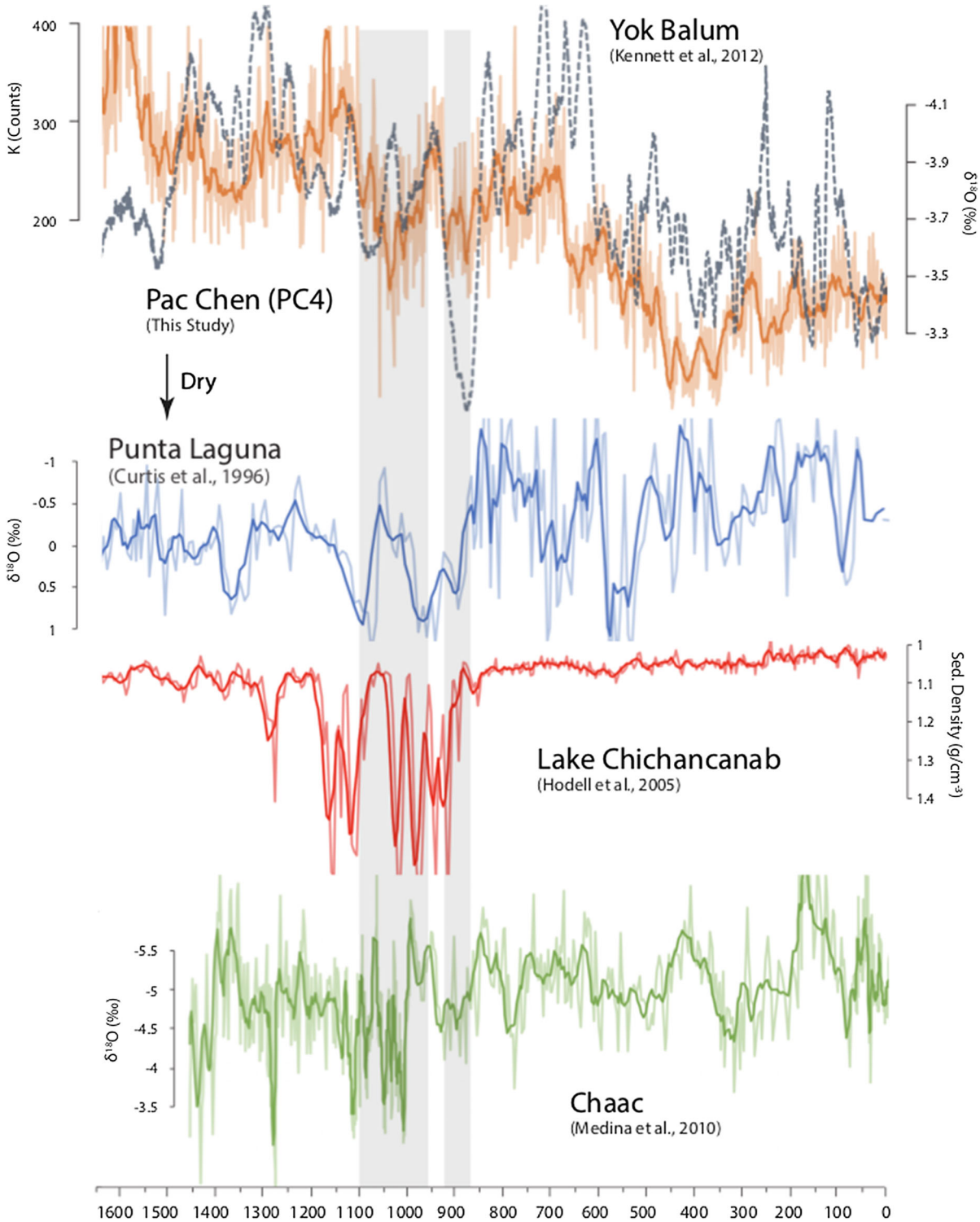
Yok Balum
(Kennett et al., 2012)
K (Counts)
400
300
200
δ18O (‰)
-4.1
-3.9
-3.7
-3.5
-3.3
Pac Chen (PC4)
(This Study)
Dry
Punta Laguna
(Curtis et al., 1996)
δ18O (‰)
-1
-0.5
0
0.5
1
Lake Chichancanab
(Hodell et al., 2005)
Sed. Density (g/cm-3)
1
1.1
1.2
1.3
1.4
Chaac
(Medina et al., 2010)
δ18O (‰)
-5.5
-5
-4.5
-4
-3.5
1600 1500 1400 1300 1200 1100 1000 900 800 700 600 500 400 300 200 100 0

◀**Fig. 8** Comparison of PC4 potassium record (cal yr BP; μXRF total counts—orange) with paleoclimate records from Yok Balum speleothem ($\delta^{18}O$—dashed grey; Kennett et al. 2012), Punta Laguna ($\delta^{18}O$—blue; Curtis et al. 1996), Lake Chichancanab (sediment density—red; Hodell et al. 2005a), Chaac speleothem ($\delta^{18}O$—green; Medina-Elizalde et al. 2010). Grey boxes denote dry periods as defined by rapid drops followed by rapid increases in K from PC4. (Color figure online)

source, so most of the Fe oxyhydroxides deposited in the lake basin originate from dissolution of limestone and aeolian dust (Norris and Röhl 1999). Potassium also has a similar source but can also be secondarily concentrated in plant material. It would be expected to behave similarly during wet periods, with increased OM decay and input to the lake basin with increased runoff from the land surface (Steinke et al. 1993). McNeill-Jewer et al. (2019) found that potassium measured in bi-annually collected sediment traps was a good indicator of rainfall in the nearby Yax Chen cave system.

The K record from PC4 spanning the last 1600 yr BP shows an overall decreasing trend, and based on the previous discussion, a trend towards drier conditions with an inflexion point at ~ 650 yr BP. Proxy records from other nearby locations on the Yucatan do not show this overall trend, neither the Chaac speleothem (Medina-Elizalde et al. 2010), nor the Punta Laguna or Lake Chichancanab records (Curtis et al. 1996; Hodell et al. 2005a), although the Punta Laguna record does show highly variable and low $\delta^{18}O$ values from ~ 950 yr BP to present (Fig. 8). The Yok Balum speleothem from Belize has the best correspondence with Pac Chen K trend showing an overall drying, but also an inflection point at 600 yr BP (Kennett et al. 2012). It doesn't appear that this K trend is significantly affected by matrix effects associated with μXRF analysis as discussed previously.

During the Classic Maya droughts (1200–850 yr BP), there is also several rapid drops in K values from ~ 1100–975 to 925–875 yr BP that span the Terminal Classic to Early Postclassic transition (~ 900 yr BP). The decrease in K is between ~ 55 and 45 cm in PC4, which does overlap the gastropod layer between ~ 50 and 40 cm, so there may be a slight matrix affect with these values (ESM4). However, the reduction in K between 50 and 45 cm which is in the marly sediment below the gastropod layer indicates that the lower values is a primary signal, as opposed to a matrix effect (ESM4). These lower K values match the droughts recorded in Punta Laguna at ~ 1150 to 950 yr BP and Lake Chichancanab at ~ 1200 to 900 yr BP which record changing water chemistry ($\delta^{18}O$ and gypsum/sediment density g cm^{-3}; Curtis et al. 1996; Hodell et al. 2005a). These proxies may be more responsive to short-term variations versus weathering and eventual input of K and Fe through runoff into the lake basin, although the density record in Lake Chichancanab is a binary record, responding once the evaporative threshold for gypsum precipitation has been reached, and thus would record extreme dry periods. The nearby Punta Laguna $\delta^{18}O$ would be more sensitive over a wider range of evaporative change than the gypsum, but both of these records show two drought phases like that of Pac Chen, albeit with offsets in timing (~ 50 years; Fig. 8; Curtis et al. 1996; Hodell et al. 2005a). The speleothem $\delta^{18}O$ records which will be sensitive and high resolution, show some similarity as well, with droughts coinciding with the Pac Chen dry period as defined by our K record (Medina-Elizalde et al. 2010; Kennett et al. 2012).

Overall, K and Fe show good correspondence with the previously established drought records but are perhaps not as sensitive for recording temporal changes. Slight differences in age for the drought period can be attributed to inaccuracies in radiometric dating of the various proxies (i.e. sediment and speleothem) and their individual sensitivities in recording environmental change (Hodell et al. 2005a). However, μXRF core scanning of shallow lake sediments does show potential, even if it may not be as sensitive as other proxies. This is because it can provide additional information on weathering inputs of terrigenous sediment into the lake basin which may provide additional insight on the droughts, but also anthropogenic effects of Maya forest clearing and agriculture in other settings (Torrescano-Valle and Islebe 2015; Battistel et al. 2018).

Conclusions

This study documenting the deep basin and shallow margin stratigraphy of Pac Chen shows that water level is mostly controlled by rising Holocene sea level and thus the lake is connected to the aquifer. Water column characteristics (temperature, conductivity)

and water depth monitoring (tidal influence) both reinforce this interpretation, but also suggest that the lake is hydrologically isolated, thus recording environmental change. This isolation from the aquifer however, may have changed through the flooding progression. The connection with the aquifer, coupled with a lack of stratigraphic evidence, indicates that there was little, to no lake drawdown during the Classic Maya droughts, because marine water intrusion from the coast would replace the reduced amount of freshwater thus keeping water level near its original position.

The shallow margin cores (PC4) also show reduced terrigenous weathering inputs (K, Fe) with the Classic Maya Droughts that match other paleoclimatic records from nearby lakes and speleothem. However, these weathering proxy indicators (K, Fe) likely have lags in their production and transport which may not record short-term changes in rainfall. Despite this limitation, the advantages of μXRF core scanning in terms of its high-resolution and efficacy presents opportunities for greater temporal and spatial coverage of the Maya droughts that may prove worthwhile in future studies.

Acknowledgements The authors would like to thank Zero Gravity Dive Center and the Mexican Cave Exploration Project for dive support and logistics (esp. Fred Devos and Christophe LeMaillot). Special thanks to the owner Carlos Marín and Fabián Arriaga of Alltournative SA de CV for allowing access to the Pac Chen facility. Funding was provided by National Sciences and Engineering Research Council of Canada Discovery Grants (EGR—RGPIN/05725-2015, MS—RGPIN/37157-2015), National Science Foundation (Grant No. 1703087) and Canada Foundation for Innovation John R. Evans Leaders Fund (EGR—105-04523).

References

Anselmetti FS, Ariztegui D, Hodell DA, Hillesheim MB, Brenner M, Gilli A, McKenzie JA, Mueller AD (2006) Late Quaternary climate-induced lake level variations in Lake Peten Itza, Guatemala, inferred from seismic stratigraphic analysis. Palaeogeogr Palaeoclimatol Palaeoecol 230:52–69

Battistel D, Roman M, Marchetti A, Kehrwald N, Radaelli M, Balliana E, Toscano G, Barbante C (2018) Anthropogenic impact in the Maya Lowlands of Petén, Guatemala, during the last 5500 years. J Quat Sci 33:166–176

Bauer-Gottwein P, Gondwe BRN, Charvet G, Marin LE, Rebolledo-Vieyra M, Merediz-Alonso G (2011) Review: the Yucatan Peninsula karst aquifer, Mexico. J Hydrol 19:507–524

Beddows PA (2004) Groundwater hydrology of a coastal conduit carbonate aquifer: Caribbean coast of the Yucatán Peninsula, México (Doctoral dissertation, University of Bristol)

Beddows P, Smart P, Whitaker F, Smith S (2007) Decoupled fresh-saline groundwater circulation of a coastal carbonate aquifer: spatial patterns of temperature and specific electrical conductivity. J Hydrol 346:18–32

Blaauw M, Christen JA (2011) Flexible paleoclimate age-depth models using an autoregressive gamma process. Bayesian Anal 6:457–474

Brenner M, Hodell D, Curtis J, Rosenmeier M, Binford M, Abbott M (2001) Abrupt climate change and pre-Columbian cultural collapse. In: Marvgraf V (ed) Interhemispheric climate linkages. Academic Press, San Diego, pp 87–103

Brenner M, Rosenmeier M, Hodell D, Curtis J (2002) Paleolimnology of the Maya Lowlands: long-term perspectives on interactions among climate, environment, and humans. Anc Mesoam 13:141–157

Collins S, Reinhardt E, Rissolo D, Chatters J, Nava Blank A, Luna Erreguerena P (2015) Reconstructing water level in Hoyo Negro, Quintana Roo, Mexico, implications for early Paleoamerican and faunal access. Quat Sci Rev 124:68–83

Costanza R, Graumlich L, Steffen W, Crumley C, Dearing J, Hibbard K, Leemans R, Redman C, Schimel D (2009) Sustainability or collapse: What can we learn from integrating the history of humans and the rest of nature? Ambio 36:522–527

Coutino A, Statsna M, Kovacs S, Reinhardt E (2017) Hurricanes Ingrid and Manuel (2013) and their impact on the salinity of the Meteoric Water Mass, Quintana Roo, Mexico. J Hydrol 551:715–729

Curtis J, Hodell D, Brenner M (1996) Climate variability on the Yucatan Peninsula (Mexico) during the past 3500 years, and implications for Maya cultural evolution. J Quat Res 46:37–47

Douglas PMJ, Brenner M, Curtis JH (2016) Methods and future directions for paleoclimatology in the Maya Lowlands. Glob Planet Change 138:3–24

Fetter CW (1988) Applied hydrogeology. Merrill Publishing Company, Columbus

Gabriel J, Reinhardt E, Peros M, Davidson D, van Hengstum P, Beddows P (2008) Paleoenvironmental evolution of Cenote Aktun Ha (Carwash) on the Yucatan Peninsula, Mexico and its response to Holocene sea-level rise. J Paleolimnol 42:199–213

Gregory B, Reinhardt E, Gifford J (2017a) The influence of morphology on sinkhole sedimentation at Little Salt Spring, Florida. J Coast Res 33:359–371

Gregory BRB, Reinhardt EG, Macumber AL, Nasser NA, Patterson T, Kovacs SE, Galloway JM (2017b) Sequential sample reservoirs for Itrax-XRF analysis of discrete samples. J Paleolimnol 57:287–293

Hastenrath S, Polzin D (2013) Climatic variations in Central America and the Caribbean. Int J Climatol 33:1348–1356

Hillesheim MB, Hodell DA, Leyden BW, Brenner M, Curtis JH, Anselmetti FS, Ariztegui D, Buck DG, Guilderson TP, Rosenmeier MF, Schnurrenberger DW (2005) Lowland neotropical climate change during the late deglacial and early Holocene. J Quat Sci 20:363–376

Hodell D, Curtis J, Brenner M (1995) Possible role of climate in the collapse of Classic Maya civilization. Nature 375:391–394

Hodell D, Brenner M, Curtis J (2005a) Terminal classic drought in the northern Maya lowlands inferred from multiple sediment cores in Lake Chichancanab (Mexico). Quat Sci Rev 24:1413–1427

Hodell D, Brenner M, Curtis J, Medina-Gonzales R, Ildefonso-Chan Can E, Albornaz-Pat A, Guilderson T (2005b) Climate change on the Yucatan Peninsula during the Little Ice Age. Quat Res 63:109–121

Jouve G, Francus P, Lamoureux S, Provencher-Nolet L, Hanh A, Habberzettl T, Fortin D, Nuttin L, The PASADO, Team Science (2013) Microsedimentological characterization using image analysis and m-XRF as indicators of sedimentary processes and climate changes during Lateglacial at Laguna Potrok Aike, Santa Cruz, Argentina. Quat Sci Rev 71:191–204

Kennett D, Brietenbach S, Aquino V, Asmerom Y, Awe J, Baldini J, Bartlein P, Culleton B, Ebert C, Jazwa C, Macri M, Marwan N, Polyak V, Prufer K, Ridlel H, Sodemann H, Winterhalder B, Haug G (2012) Development and disintegration of Maya political systems in response to climate change. Science 338:788–791

Khan N, Ashe E, Horton B, Dutton A, Kopp R, Brocard G, Englehart S, Hill D, Peltier W, Vane C, Scatena F (2017) Drivers of Holocene sea-level change in the Caribbean. Quat Sci Rev 155:13–36

Kovacs S, Reinhardt E, Chatters J, Rissolo D, Schwarcz H, Collins S, Kim ST, Nava Blank A, Luna Erreguerena P (2017a) Calcite raft geochemistry as a hydrological proxy for Holocene aquifer conditions in Hoyo Negro and Ich Balam (Sac Actun Cave System), Quintana Roo, Mexico. Quat Sci Rev 10:205–214

Kovacs S, Reinhardt E, Statsna M, Coutino A, Werner C, Collins S, Devos F, Le Maillot C (2017b) Hurricane Ingrid and Tropical Storm Hanna's effects on the salinity of the coastal aquifer, Quintana Roo, Mexico. J Hydrol 551:704–714

Kovacs S, Reinhardt E, Werner C, Kim ST, Devos F, Le Maillot C (2018) Seasonal trends in calcite-raft precipitation from cenotes Rainbow, Feno and Monkey Dust, Quintana Roo, Mexico: implications for paleoenvironmental studies. Palaeogeogr Palaeoclimatol Palaeoecol 497:157–167

Leyden B, Brenner M, Dahlin B (1998) Cultural and climatic history of Coba, a Lowland Maya City in Quintana Roo, Mexico. Quat Res 49:111–122

McNeill-Jewer CA, Reinhardt EG, Collins S, Kovacs S, Chan WM, Devos F, LeMaillot C (2019) The effect of seasonal rainfall on nutrient input and biological productivity in the Yax Chen cave system (Ox Bel Ha), Mexico, and implications for μXRF core studies of paleohydrology. Palaeogeogr Palaeoclimatol Palaeoecol 534:109289

Medina-Elizalde M, Burns S, Lea D, Asmerom Y, von Gunten L, Polyak V, Vuille M, Karmalkar A (2010) High resolution stalagmite climate record from the Yucatan Peninsula spanning the Maya terminal classic period. Earth Planet Sci Lett 298:255–262

Metcalfe S, Barron J, Davies S (2015) The Holocene history of the North American Monsoon: 'known knowns' and 'known unknowns' in understanding its spatial and temporal complexity. Quat Sci Rev 120:1–27

Moseley GE, Richards DA, Smart PL, Standish CD, Hoffmann DL, ten Vinn O (2015) Early–middle Holocene relative sea-level oscillation events recorded in a submerged speleothem from the Yucatán Peninsula, Mexico. Holocene 25:1–11

Negreros-Castillo P, Snook L, Mize C (2003) Regenerating mahogany (*Sweietenia macrophyllia*) from seed in Quintana Roo, Mexico: the effects of sowing method and clearing treatment. For Ecol Manag 183:351–362

Norris RD, Röhl U (1999) Carbon cycling and chronology of climate warming during the Palaeocene/Eocene transition. Nature 401:775

Null KA, Knee KL, Crook ED, de Sieyes NR, Rebolledo-Vieyra M, Hernández-Terrones L, Paytan A (2014) Composition and fluxes of submarine groundwater along the Caribbean coast of the Yucatan Peninsula. Cont Shelf Res 77:38–50

Parra SM, Valle-Levinson A, Marino-Tapia I, Enriquez C (2015) Salt intrusion at a submarine spring in a fringing reef lagoon. J Geophys Res C Oceans 120:2736–2750

Pérez L, Bugja R, Massaferro J, Steeb P, van Geldern R, Frenzel P, Brenner M, Scharf B, Schwalb A (2010) Post-Columbian environmental history of Lago Petén Itzá, Guatemala. Revista Mexicana de Ciencias Geológicas 27:490–507

Perry E, Velazquez-Oliman G, Socki RA (2003) Hydrogeology of the Yucatán Peninsula. In: Gomez-Pompa A, Allen MF, Fedick SL, Jimenez-Osornio JJ (eds) The lowland Maya: three millennia at the human–wildland interface. Haworth, Binghamton, pp 115–138

Perry E, Paytan A, Pedersen B, Velazquez-Oliman G (2009) Groundwater geochemistry of the Yucatan Peninsula, Mexico; constraints on stratigraphy and hydrogeology. J Hydrol 367:27–40

Regalado IS, García SL, Alvarado LP, Caballero M, Vázquez AL (2018) Ecological drivers of testate amoeba diversity in tropical water bodies of central Mexico. J Limnol 77:385–399

Reimer PJ, Bard MGL, Bayliss A, Beck JW, Blackwell PG, Ramsey CB, Buck CE, Edwards RL, Freidrich M, Groots PM, Guilderson TP, Haflidason H, Hajdas I, Hatté C, Heaton TJ, Hoffmann DL, Hogg AG, Hughen KA, Kaiser KF, Kromer B, Manning SW, Nui M, Reimer RW, Richards DA, Scott EM, Southon JR, Turney CSM, van der Plicht J (2013) IntCal13 and Marine13 radiocarbon age calibration curves, 0–50,000 years Cal BP. Radiocarbon 55:1887–1896

Rosenmeier MF, Brenner M, Hodell DA, Martin JB, Curtis JH, Binford MW (2016) A model of the 4000-year paleohydrology ($\delta^{18}O$) record from Lake Salpetén, Guatemala. Glob Planet Change 138:43–55

Smart PL, Beddows PA, Doerr S, Smith SL, Whitaker FF (2006) Cave development on the Caribbean coast of the Yucatan Peninsula, Quintana Roo, Mexico. Geol Soc Am Spec Pap 404:105–128

Schneider T, Bischoff T, Haug GH (2014) Migrations and dynamics of the intertropical convergence zone. Nature 513:45–53

Steinke TD, Holland AJ, Singh Y (1993) Leaching losses during decomposition of mangrove leaf litter. S Afr J Bot 59:21–25

Stinnesbeck W, Becker J, Hering F, Frey E, Gonzalez AG, Fohlmeister J et al (2017) The earliest settlers of Mesoamerica date back to the late Pleistocene. PLoS ONE 12(8):e0183345

Talley L, Pickard G, Emery W, Swift J (2011) Gravity waves, tides, and coastal oceonography. Descriptive physical oceanography: an introduction. Academic Press, Cambridge, pp 223–244

Torrescano N, Islebe G (2006) Tropical forest and mangrove history from southeastern Mexico: A 5000 yr pollen record and implications for sea level rise. Veg Hist Archaeobot 15:191–195.

Torrescano-Valle N, Islebe G (2015) Holocene paleoecology, climate history and human influence in the southwestern Yucatan Peninsula. Rev Palaeobot Palynol 217:1–8

Valle-Levinson A, Marino-Tapia I, Enriquez C, Waterhouse AF (2011) Tidal variability of salinity and velocity fields related to intense point-source submarine groundwater discharges into the coastal ocean. Limnol Oceanogr 56:1213–1224

van Hengstum P, Reinhardt E, Beddows P, Huang R, Gabriel J (2008) Thecamoebians (Testate Amoebae) and foraminifera from three anchialine cenotes in Mexico: low salinity (1.5–4.5 psu) faunal transitions. J Foraminifer Res 38:305–317

van Hengstum P, Reinhardt E, Beddows P, Gabriel J (2010) Linkages between Holocene paleoclimate and paleohydrology preserved in a Yucatan underwater cave. Quat Sci Rev 29:2788–2798

Van Hengstum P, Maale G, Donnelly J, Albury N, Onac B, Sullivan R, Winkler T, Tamalavage A, MacDonald D (2018) Drought in the northern Bahamas from 3300 to 2500 years ago. Quat Sci Rev 186:169–185.

Ward W, Weidi A, Back W (1985) Geology and hydrogeology of the Yucatan and Quaternary geology of Northeastern Yucatan Peninsula. New Orleans Geological Society, New Orleans